Original Article
Cite This: Colloid & Nanoscience Journal 1 (2023) 163-172.
CNJ.araku.ac.ir

# Neuro-fuzzy logic system for prediction of dye removal from aqueous solutions by a polymeric nanocomposite

**Keyvandokht Suratgar[1*], Amir Abolfazl Suratgar[2]**

**Received:**2023-10-25
**Revised:** 2023-12-09
**Accepted:** 2023-12-11
DOI: **10.61186/CNJ.1.3.163**

[1]Iranian Academic for Education Culture and Research, Nano Research Center, Markazi province, 38158-9-9989, Iran

[2]Distributed Intelligent Optimization Research Laboratory, Department of Electrical Engineering, Amirkabir University of Technology, Tehran, Iran

**Abstract**

Here we explain the successful synthesis of a new polymeric nanocomposite and study the removal of a cationic dye, brilliant green, from aqueous solutions. The nanocomposite is characterized by scanning electron microscopy (SEM) and X-ray diffraction (XRD). In addition, adsorption kinetics and effects of various variables such as solution pH, adsorbent mass, and initial dye concentration are investigated. Moreover, the fuzzy model is used to investigate the dye removal efficiency. The investigation of the results obtained using the fuzzy model shows that it is suitable for the prediction of dye adsorption onto nanocomposite. The coefficient of determination ($R^2$) and mean squared error (MSE) for the optimal model were obtained to be 0.9981 and 0.1538, respectively. The equilibrium experimental data are represented by Langmuir, Freundlich, and Sips isotherms. Results briefly indicate that adsorption of dye by nanocomposite obeys Langmuir isotherm and pseudo-second-order kinetic model.

**Keywords:** Dye removal, Polymeric nanocomposite, Neuro-Fuzzy modeling

## 1. Introduction

Brilliant green (BG) is a triphenylmethane dye, originally used as a dye in wool, silk, and jute and in leather cotton, paper, and acrylic industries, has also been widely used in the fish farming industry for many years. However, BG has become a highly controversial compound due to its effects on the reproductive and immune systems and its carcinogenic and genotoxic properties [1-2]. To date, various methods include physicochemical, chemical, and biological methods, such as flocculation, precipitation, coagulation, membrane filtration, adsorption, electrochemical techniques, ozonation, and fungal decolorization are used for removing dyes from wastewater [3]. Adsorption is widely used for the removal of pollutants from wastewater [4, 5]. Recently, magnetic nanoparticles have attracted attention because of their special properties such as their low toxicity, high dispersibility in water, easiness of surface modification, easy separation, and superparamagnetic properties [6-8].
It is therefore essential to make a new type of nanocomposite with enhanced capacity for dye pollutants removal [9-14] and also can be used as an antibacterial agent [15-17].

The purpose of the present study is to indicate the feasibility of a new magnetic and polymeric nanocomposite that can remove BG from aqueous solutions. Since the ability of sorbents to remove pollutants is strongly influenced by parameters such as pH, time, temperature, initial concentration of pollutants, and sorbent mass, it is, therefore, essential to use an appropriate approach for maximizing the removal efficiency of pollutants by adsorbents. The complexity, fuzziness, and uncertainty existent in addition to the non-linear behavior of most effective variables need a powerful tool to overcome these problems. Nowadays, intelligent techniques such as artificial neural networks (ANN), fuzzy logic (FL), and genetic algorithms (GA) have been used in water treatment applications [2,18-20].
Neural fuzzy systems can be a more versatile approach to the prediction of dye removal properties. Combination of the explicit knowledge representation of fuzzy logic with the learning power of neural nets can be more useful [21].
This study is aimed at the following objectives for the first time:
1. Suggest a novel, simple yet accurate fuzzy neural system to estimate dye removal.
2. Testing the performance of the model for dye removal prediction.
In addition, the adsorption isotherms like Langmuir and Freundlich models were studied for the sorption behavior of this new sorbent-based on the polymer nanocomposite. The prepared nanocomposite was characterized with Powder X-ray diffraction (XRD) and Field emission scanning electron microscopy (FE-SEM) and was used for dye removal as an application in wastewater treatment field.



Corresponding Authors: Keyvandokht Suratgar
suratgar.qnn@gmail.com

## 2. Experimental Investigation

### 2.1. Materials

All chemicals were purchased from Merck (Darmstadt, Germany) and were used without further purification. Stock solutions of BG were prepared by dissolving appropriate amounts of dye in distilled water.

**Table 1**. The properties of the commercial CuO nanoparticles.

| Density (g/ml) | Colore | Shape | Size (nm) | Purity (%) | Nanoparticle |
|---|---|---|---|---|---|
| 6.35 | black | spherical | 55-65 | 99.95 | Copper (II) oxide |

### 2.2. Preparation of nanofluid

$Fe_3O_4$ nanoparticles were prepared by chemical co-precipitation method [7]. Briefly, $FeCl_2{\cdot}4H_2O$ (2.25 g) and $FeCl_3{\cdot}6H_2O$ (8.48 g) were dissolved in 400 mL deionized water under nitrogen atmosphere with vigorous stirring (1000 rpm) at 80 °C for 20 min. Then, 20 mL ammonia solution (25 % wt) was added to the solution. The color of solution immediately became black. Then, 2 g $Fe_3O_4$, 8 mmol methyl methacrylate as functional monomer, 40 mmol ethylenglycoldimethacrylate as cross-linker, and 20 mg azobisisobutyronitrile as initiator were dissolved in 60 mL DMSO and mixed well, then the solution was purged with nitrogen gas for about 30 min to remove oxygen which inhibited polymerization and then sealed under nitrogen gas. Polymerization was carried out in a water bath at 60°C for 12 h. The obtained polymer was collected and washed with acetone. Then the polymer dried at 40°C under a vacuum.

### 2.3. Characterization

The particle size and morphology of the nanocomposite were determined by a scanning electron microscope model TESCAN Vega instrument. In addition, an X-ray diffraction (XRD) pattern of the $Fe_3O_4$ nanoparticles was recorded using a Philips X-ray diffractometer (model PW 3040/60 X'pert pro). The data were processed on a Pentium IV computer with programs written in MATLAB 6.5 on Windows.

### 2.4. Procedure

For each experiment, 10 ml of dye solution of known concentrations, pH, and the known amount of nanocomposite were taken in a 100-ml Pyrex glass Erlenmeyer flask. After the shaking, the supernatant was collected for determination of the dye concentration. The analysis of dye was performed by a UV–Vis spectrophotometer (Analytikjena SPECORD250). A Metrohm 744 pH meter (Metrohm, Switzerland) was used for pH adjustments.

The removal percentage (R%) and uptake capacity (q) was obtained according to the following equations:

$$R\% = \frac{(C_o - C_e)}{C_o} \times 100 \quad (1)$$

$$q = \frac{(C_o - C_e)V}{m} \quad (2)$$

where $C_o$ and $C_e$ are the initial and equilibrium concentrations of the dye in the solutions, respectively, V is the volume of solution (L) and m is the sorbent mass (g) [22,23].

### 2.5. Fuzzy logic

The idea of fuzzy logic was first advanced by Dr. Lotfi Zadeh of the University of California at Berkeley in the 1960s. Basically, fuzzy logic is a multi-valued logic that allows intermediate values to be defined between conventional evaluations like true/false, yes/no, high/low, etc. Notions like rather tall or very fast can be formulated mathematically and processed by computers, in order to apply a more human-like way of thinking in the programming of computers. An inherent vagueness is present in our natural language when we describe phenomena that do not have abrupt boundaries. Fuzzy sets are mathematical objects modeling this impreciseness. Fuzzy set theory provides a mathematical tool for carrying out approximate reasoning processes when available information is uncertain, incomplete, or vague. Fuzzy logic converts the complex problem into simpler problems using approximate reasoning. The system is described by fuzzy rules and membership functions using human-type language and linguistic variables. A fuzzy set is a collection of ordered pairs A={x, μ(x)} that describes the relationship between an uncertain quantity x and a membership function μ(x), where μ (x) is a number between 0 and 1. The fuzzy model formulates the information on an intensity scale. Rules, fuzzy inference engine, fuzzifier, and defuzzifier are four elements of a fuzzy model [24-26].

## 2.6. Artificial neural networks

An artificial neural network (ANN) is composed of simple computational units (neurons), which are inspired by the biological nervous system (brain). One of the most popular ANN architectures (topology) is a multi-layer feed-forward network. The network consists of three sequentially connected segments: the input layer, one or more hidden layers, and the output layer. ANNs are high-performance, non-linear analytical methods, that can exhibit the relationship between input/output variables without prior knowledge of the correlation between the variables involved in the system [18-21]. Each neuron of the neural network is connected to others using direct connection links, each with associated weight, which represents information being used by the net to solve the problem (Fig. 1). The output of a neuron is computed from the following Eq:

$$O_j = f\left(\sum_{i=1}^{n} W_{ji} * x_i + b_j\right) \quad (3)$$

where $O_j$=output of jth neuron, f =activation or transfer function, $b_j$=bias of jth neuron, $w_{ji}$=synaptic weight corresponding to the ith synapse of jth neuron, $x_i$=ith input signals to jth neuron.

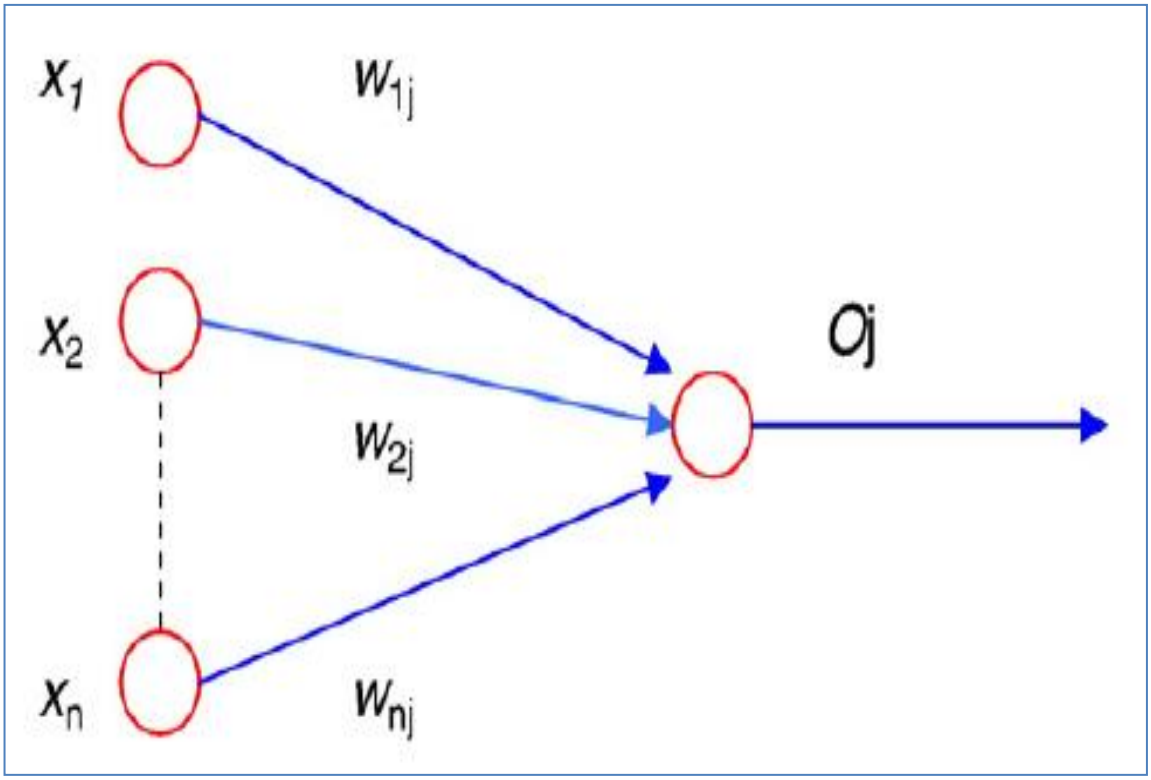


**Fig 1.** A simple neuron.

## 2.7. Neuro-fuzzy systems

Neuro-fuzzy systems (NFS) refer to combinations of artificial neural networks and fuzzy logic in the field of artificial intelligence, which was proposed by Jang in 1993. The basic idea behind this NFS is that it combines the human-like reasoning style of fuzzy systems with the learning and connectionist structure of neural networks. NFS provides powerful and flexible universal approximations with the ability to explore interpretable IF-THEN rules. The use of NFS is proliferating in many sectors of our social and technological life. A combination of fuzzy logic with the learning power of neural nets can reduce the problems associated with each of these techniques [27].

# 3. Results and discussion

## 3.1. XRD and FESEM study

The XRD pattern of $Fe_3O_4$ nanoparticles is shown in Fig. 2. Six characteristic peaks for $Fe_3O_4$ ($2\theta$ = 30.1°, 35.5°, 43.3°, 53.4°, 57.2° and 62.5°), respectively, corresponding to indices (220), (311), (400), (422), (511), and (440) are

observed in the pattern [28-30]. The size and morphology of the resultant nanocomposite were determined by FESEM. As shown in Fig. 3, the nanoparticles have a nearly spherical shape with a smooth and uniform surface morphology.

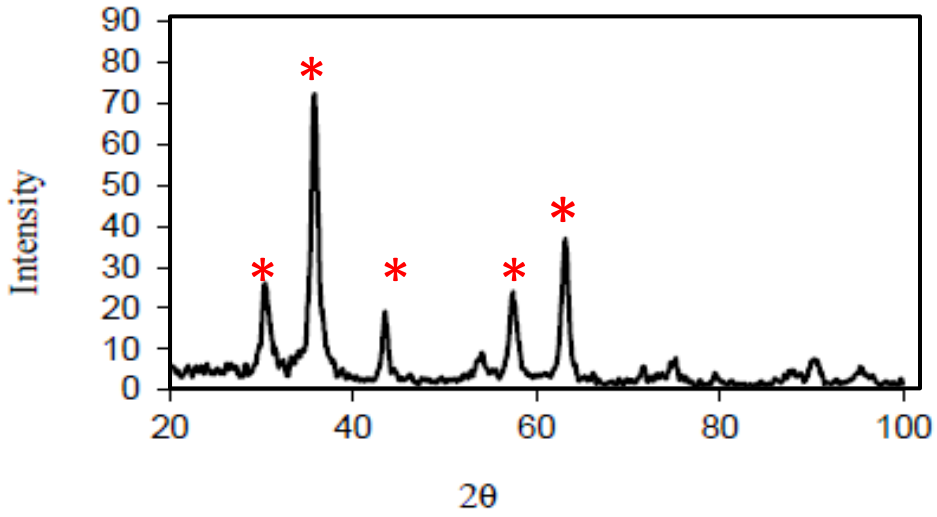


**Fig. 2.** The XRD pattern of $Fe_3O_4$ nanoparticles.

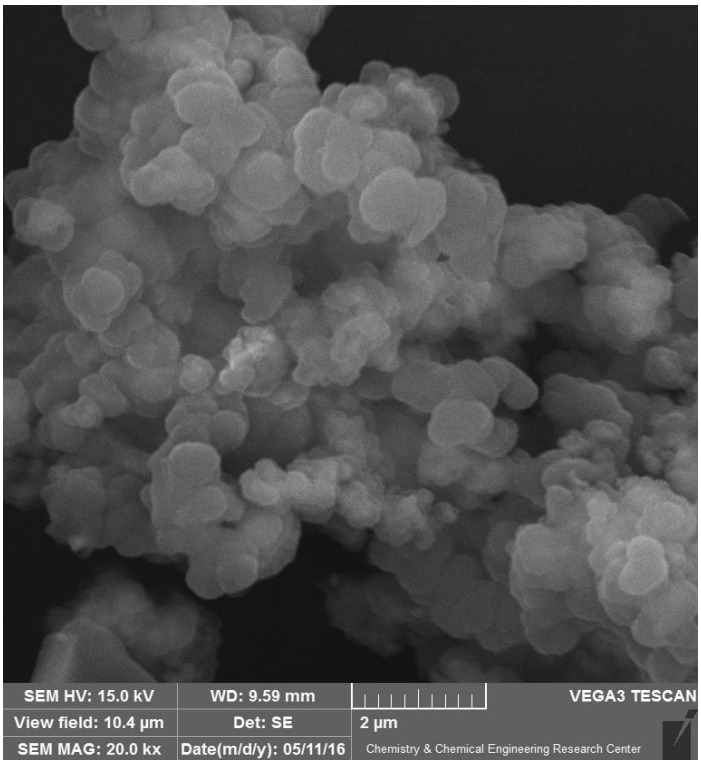


Fig 3. FESEM image of the nanocomposite at 40,000 × magnification.

## 3.2. Data acquisition and processing

In this process, a series of experiments were undertaken at various amounts of adsorbent from 0.02–0.1g, different BG concentrations in the range of 100–1000 mg/L, the pH in the range of 4 – 10, and time in the range of 4 – 60 min (Table 1). In this study, NFS is applied to predict the removal efficiency of BG by a nanocomposite. The Neural Network code of MATLAB (R2012a) mathematical software was used to predict BG removal efficiency. In this

study, four neurons in the input layer (pH, $C_{BG}$ (concentration of BG), time, and m (sorbent mass)) and one neuron ($\%R_{BG}$) in the output layer were applied. All the data (input and output) for NFS models were normalized between 0 and 1 to avoid numerical overflows due to very large or small weights. The normalization equation applied is as follows:

$$y = \frac{x_i - x_{min}}{x_{max} - x_{min}} \quad (4)$$

where y is the normalized value of $x_i$, and the $x_{max}$ and $x_{min}$ are the maximum and minimum value of $x_i$, respectively. The experimental and predicted removal percentages (%RBG) are shown in Table 1. In this regard, comparison criteria are needed to quantify the difference between responses predicted by the NFS and the actual values. To evaluate the performance of the constructed NFS, some useful statistical criteria which are the root mean square error of prediction (RMSEP), mean squared error (MSE) relative standard error of prediction (REP) and coefficient of determination ($R^2$) were used [31, 32]:

$$RMSEP = \sqrt{\frac{\sum_{i=1}^{n}(x_i - \hat{x}_i)^2}{n}} \quad (5)$$

$$REP = 100\sqrt{\frac{\sum_{j=1}^{n}(x_i - \hat{x}_i)^2}{\sum_{j=1}^{n} x_i^2}} \quad (6)$$

$$R^2 = 1 - \frac{\sum_{i=1}^{n}(\hat{x}_i - x_i)^2}{\sum_{i=1}^{n}(\hat{x}_i - \bar{x}_i)} \quad (7)$$

$$MSE = \frac{1}{n}\sum_{i=1}^{n}(x_i - \hat{x}_i)^2 \quad (8)$$

where $x_i$ was the predicted value of model, $\hat{x}_i$ as the experimental value, n was the number of data and $\bar{x}_i$ is the average of the actual values.

The RMSEP and REP values for NFS were found as 0.39 and 0.84, respectively. $R^2$ value for NFS was found as 0.9981. $R^2$ provides a measure of how well the investigated model can predict the future results. However, these results indicate predictive ability of NFS for prediction of dye removal efficiency.

**Table 1.** Isotherm parameters values for the adsorption of BG on nanocomposite.

| Sample | pH | m (g) | C (mg/L) | T (min) | $\%R_{Exp}$ | $\%R_{Pred}$ |
|---|---|---|---|---|---|---|
| 1 | 4 | 0.02 | 550 | 32 | 16 | 16.05 |
| 2 | 10 | 0.02 | 550 | 32 | 34 | 34.85 |
| 3 | 4 | 0.1 | 550 | 32 | 68 | 68.01 |
| 4 | 10 | 0.1 | 550 | 32 | 85 | 85.08 |
| 5 | 7 | 0.06 | 100 | 4 | 18 | 18.16 |
| 6 | 7 | 0.06 | 1000 | 4 | 5 | 5.0 |
| 7 | 7 | 0.06 | 100 | 60 | 67 | 67.89 |
| 8 | 7 | 0.06 | 1000 | 60 | 13 | 13.11 |
| 9 | 4 | 0.06 | 100 | 32 | 37 | 37.6 |
| 10 | 10 | 0.06 | 100 | 32 | 64 | 64.0 |
| 11 | 4 | 0.06 | 1000 | 32 | 13 | 13.8 |
| 12 | 10 | 0.06 | 1000 | 32 | 23 | 23.23 |
| 13 | 7 | 0.02 | 550 | 4 | 6 | 6.0 |
| 14 | 7 | 0.1 | 550 | 4 | 49 | 49.69 |
| 15 | 7 | 0.02 | 550 | 60 | 25 | 25.35 |
| 16 | 7 | 0.1 | 550 | 60 | 83 | 83.0 |
| 17 | 4 | 0.06 | 550 | 4 | 15 | 15.29 |
| 18 | 10 | 0.06 | 550 | 4 | 31 | 31.06 |
| 19 | 4 | 0.06 | 550 | 60 | 39 | 39.33 |
| 20 | 10 | 0.06 | 550 | 60 | 60 | 60.0 |
| 21 | 7 | 0.02 | 100 | 32 | 21 | 21.58 |
| 22 | 7 | 0.1 | 100 | 32 | 93 | 93.02 |
| 23 | 7 | 0.02 | 1000 | 32 | 7 | 7.07 |
| 24 | 7 | 0.1 | 1000 | 32 | 37 | 37.06 |
| 25 | 7 | 0.06 | 550 | 32 | 55 | 55.3 |

### 3.3. Equilibrium isotherms

Equilibrium data, commonly known as sorption isotherms, are basic requirements in the design of sorption systems. Therefore, the equilibrium studies were carried out at pH 8, sorbent mass of 0.08 g and contact time of 60 min. The equilibrium data were investigated by the most commonly used isotherms; Langmuir, Freundlich and Sips models [33]. The Langmuir isotherm supposes that uptake of sorbate takes place on a homogenous surface by monolayer sorption with no interaction between the sorbates. Also, all the binding sites of the surface have equal energy of sorption. The Freundlich isotherm, on the other hand, supposes a heterogeneous sorption surface with sites that have different energies of sorption. Sips isotherm is a combined form of Langmuir and Freundlich expressions deduced for predicting the heterogeneous adsorption systems and circumventing the limitation of the rising adsorbate concentration associated with Freundlich isotherm model. At low sorbate concentrations, it reduces to Freundlich isotherm; while at high concentrations, it predicts a monolayer adsorption capacity characteristic of the Langmuir isotherm [30-33].

The Langmuir, Freundlich, and Sips isotherms are represented by the following equations, respectively:

Langmuir: $$q_e = \frac{q_{max} b C_e}{1 + b C_e} \quad (9)$$

Freundlich: $$q_e = K_F\, Ce^{1/n} \quad (10)$$

Sips: $$q = \frac{q_s (b_s C_{eq})^{n_s}}{[1 + (b_s C_{eq})^{n_s}]} \quad (11)$$

Where $q_{max}$ is the maximum amount of adsorption (mg/g), $q_e$ is the adsorption capacity at equilibrium (mg/g), $C_e$ is the equilibrium concentration of sorbate in the solution (mg/L), $b$ is the adsorption equilibrium constant (L/mg), $K_F$ is the constant (mg/g) representing the adsorption capacity, and n is the constant depicting the adsorption intensity. Also, $b_s$ is the Sips constant; and $n_s$ is the constant depicting the adsorption intensity. The adsorption isotherm data are in Table. 2. The $q_e$ of the dyes was increased with increasing concentrations until reaching equilibrium.

**Table 2.** Isotherm parameters values for the adsorption of BG on nanocomposite.

| | | | | | |
|---|---|---|---|---|---|
| **Langmuir Isotherm** | | | | | |
| $q_{max}$ (mg/g) | b (L/mg) | $R^2$ | $\chi^2$ | Δq | |
| 62.6 | 0.0026 | 0.984 | 1.12 | 0.104 | |
| **Freundlich Isotherm** | | | | | |
| $k_f$ | n | $R^2$ | $\chi^2$ | Δq | |
| 1.95 | 2.21 | 0.920 | 6.8 | 0.363 | |
| **Sips Isotherm** | | | | | |
| $q_s$ | $b_s$ | $n_s$ | $R^2$ | $\chi^2$ | Δq |
| 52.8 | 0.0037 | 1.38 | 0.995 | 0.66 | 0.087 |

(10 mL solution, pH: 8 and 0.08 g of nanocomposite).

An error function is needed to compare the quality of each model. Consequently, Chi-square ($\chi^2$) test, coefficient of determination ($R^2$) and normalized standard deviation (Δq) were used as criteria to find out the best-fitted isotherm model to the experimental data in non-linear regression analysis. These error functions are given as [33].

$$\chi^2 = \sum_{i=1}^{n} \frac{(q_{e,cal} - q_{e,\exp})^2}{q_{e,\exp}} \quad (12)$$

$$R^2 = \sum (q_{e,\exp} - \bar{q}_{calc})^2 / \sum ((q_{e,\exp} - \bar{q}_{calc})^2 + (q_{e,\exp} - q_{calc})^2) \quad (13)$$

$$\Delta q = \sqrt{\frac{\sum [(q_{e,\exp} - q_{e,cal}) / q_{e,\exp}]^2}{n-1}} \quad (14)$$

where $n$ is the number of data points, $q_{e,exp}$ is the equilibrium adsorption capacity from the experiment (mg/g), and $q_{e,cal}$ is the equilibrium capacity calculated according to the dynamic model (mg/g).

From Table 1, it can be concluded that the Sips isotherm model was more appropriate for the experimental data than the others because of the high value of the correlation coefficient and low values of Δq and $\chi^2$.

### 3.4. Sorption kinetics

The effect of contact time on the removal efficiency of target dye was studied to determine the time taken by 0.06 g nanocomposite to remove dye (50 mg/g solution of 10 mL) at pH = 8. The results were shown in Fig. 4. It could be seen that the adsorption equilibrium was achieved at about 60 min. As the adsorption reached equilibrium, the adsorbent surface became inaccessible due to the repulsive forces between the adsorbed dye and those present in solution [33].

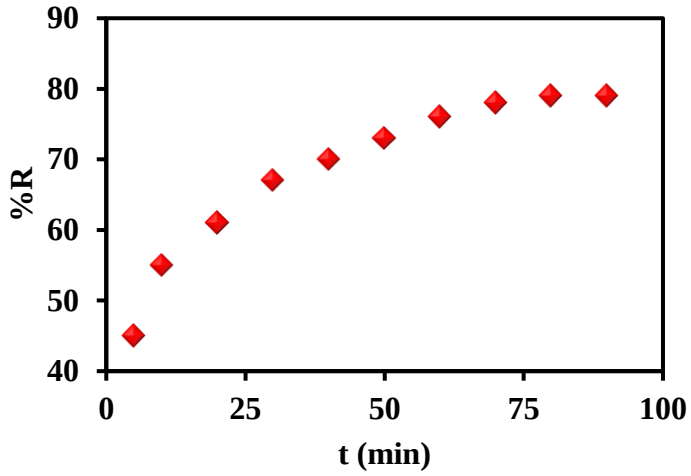


**Fig 4.** The effect of contact time on dye removal efficiency (pH = 8; m = 0.08; T = 25 °C; sample volume = 10 mL; $C_{BG}$: 200 mg/L).

Several kinetic models such as pseudo-first order, pseudo-second order and intraparticle diffusion, are available to describe the sorption kinetics [20, 21].

The pseudo-first order kinetic model can be defined as:

$$\ln(q_e - q_t) = \ln q_e - K_1 t \quad (15)$$

where $K_1$ is the pseudo-first order rate constant of sorption. The values of $q_e$ and $k_1$ can be determined from the slope and intercept of the plot obtained by plotting $\ln(q_e - q_t)$ versus t (figure not shown).

The pseudo-second order kinetic model can be represented as:

$$\frac{t}{q_t} = \frac{1}{k_2 q_2^2} + \frac{1}{q_2} t \quad (16)$$

Where $q_2$ is the maximum adsorption capacity (mg/g) for the pseudo-second-order adsorption, $q_t$ is the amount of dye adsorbed at time $t$ (mg/g), and $k_2$ is the equilibrium rate constant of pseudo-second-order adsorption (g/mg.min). The parameters calculated for the different kinetic models are listed in Table 3. As seen from the table, due to high $R^2$, the pseudo-second order is predominant kinetic model for the dye sorption by nanocomposite (Fig. 5).

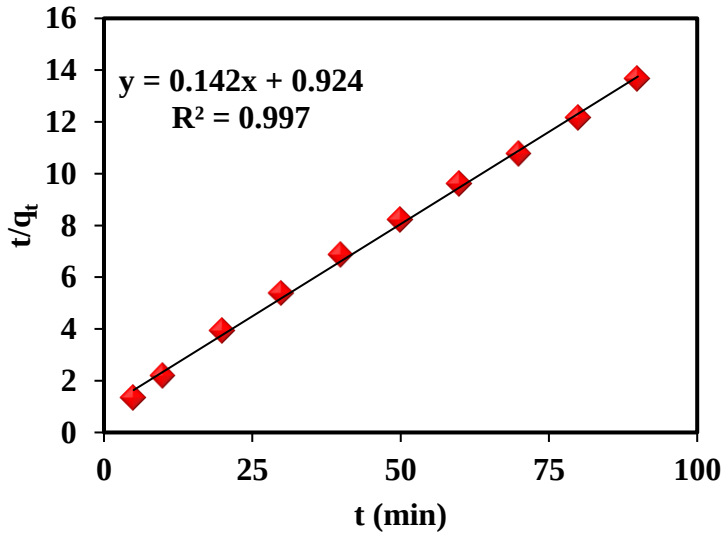


**Fig 5**. The Pseudo second order adsorption kinetics of BG onto nanocomposite.

In order to identify the diffusion mechanism, the intraparticle diffusion model can be represented as:

$q_t = k_i t^{1/2} + C$ (17)

where $k_i$ is the intraparticle diffusion rate constant and C is a constant which gives information about the thickness of boundary layer. According to this model, the plot of q versus $t^{1/2}$ yields a straight line passing through the origin if the sorption process obeys the sole intraparticle diffusion model. According to Table 3, and therefore, the intraparticle diffusion is not the only rate limiting step. It could be stated that this process is complex and may involve more than one mechanism.

**Table** 3. Kinetics constants for dye adsorption onto nanocomposite (10 mL solution, pH: 8, T: 25 °C, 0.0^ g of nanocomposite and $C_{BG}$: 200 mg/L).

| System | Pseudo-first order | | | Pseudo-second order | | | Intraparticle diffusion | | |
|---|---|---|---|---|---|---|---|---|---|
| $q_{(Exp)}$ (mg/g) | $q_{1(cal)}$ (mg/g) | $k_1$ ($min^{-1}$) | $R^2$ | $q_{2(cal)}$ (mg/g) | $k_2$ (g/mg.min) | $R^2$ | $k_p$ ($mg/g.min^{1/2}$) | C | $R^2$ |
| 6.6 | 3.19 | 0.024 | 0.983 | 7.04 | 0.022 | 0.997 | 0.135 | 3.65 | 0.924 |

## 4. Conclusions

In this paper, a new magnetic polymeric nanocomposite was successfully synthesized and used as an efficient nanosorbent to remove BG dye from aqueous solution. The investigation of the results obtained using the NFS model shows that it is suitable for the prediction of dye adsorption onto nanocomposite. The coefficient of determination ($R^2$) and mean squared error (MSE) for the optimal model were obtained to be 0.9981 and 0.1538, respectively. Equilibrium experimental data were represented by Langmuir, Freundlich and Sips isotherms and the nanocomposite exhibited high sorption capacity toward BG (q = 52.8 mg/g). Results briefly showed that adsorption of BG by nanocomposite obeys Sips isotherm. Moreover, the dye removal kinetics followed the pseudo-second-order expression.

References

## Conflicts of Interest

The author declares no conflict of interest.

## Author information

*Corresponding Author: Keyvandokht Suratgar
suratgar.qnn@gmail.com

## References

[1] J. Zolgharnein, M. Bagtash, T. Shariatmanesh. Simultaneous removal of binary mixture of Brilliant Green and Crystal Violet using derivative spectrophotometric determination, multivariate optimization and adsorption characterization of dyes on surfactant modified nano-γ-alumina. Spectrochim Acta A. 137 (2015) 1016–1028. https://doi.org/10.1016/j.saa.2014.08.115

[2] M. Ghaedi, A. Ansari, F. Bahari, A.M. Ghaedi, A Vafaei. A hybrid artificial neural network and particle swarm optimization for prediction of removal of hazardous dye brilliant green from aqueous solution using zinc sulfide nanoparticle loaded on activated carbon. Spectrochim Acta Part A. 137 (2015) 1004–1015. https://doi.org/10.1016/j.saa.2014.08.011

[3] V.G. Gupta, Suhas. Application of low-cost adsorbents for dye removal- A review. J Environ Manage. 90 (2009) 90: 2013-2042. https://doi.org/10.1016/j.jenvman.2008.11.017

[4] G. Crini. Non-conventional low-cost adsorbents for dye removal: A review. Bioresour Technol. 97 (2006) 1061–1085. https://doi.org/10.1016/j.biortech.2005.05.001

[5] J. Zolgharnein, M. Bagtash, S. Feshki, P. Zolgharnein, D. Hammond. Crossed mixture process design optimization and adsorption characterization of multi-metal (Cu(II), Zn(II) and Ni(II)) removal by modified Buxus sempervirens tree leaves. J Taiwan Inst Chem Eng. 2017 http://doi.org/10.1016/j.jtice.2017.03.020.

[6] H. Moghanian, A. Mobinikhaledi, A.G. Blackman, E. Sarough-Farahani, Sulfanilic acid-functionalized silica-coated magnetite nanoparticles as an efficient, reusable and magnetically separable catalyst for the solvent-free synthesis of 1-amido- and 1-aminoalkyl-2-naphthols. RSC Adv. 4 (2014) 28176-28185. https://doi.org/10.1039/c4ra03676j

[7] M. Bagtash, Y. Yamini, E. Tahmasebi, J. Zolgharnein, Z. Dalirnasab, Magnetite nanoparticles coated with tannic acid as a viable sorbent for solid-phase extraction of $Cd^{2+}$, $Co^{2}$+ and $Cr^{3+}$. Microchim Acta. 183 (2016) 183:449–456. https://doi.org/10.1007/s00604-015-1667-5

[8] H. Moghanian, A. Mobinikhaledi, Z. Baharangiz, Synthesis, characterization and magnetic properties of novel heat resistant polyimide nanocomposites derived from 14 Hdibenzo [a,j] xanthenes. J Polym Res. 21 (2014) 513. https://doi.org/10.1007/s10965-014-0513-5

[9] A. Salabat, F. Mirhoseini, Polymer-based nanocomposites fabricated by microemulsion method, Polym. Compos. 43 (2022) 1282–94. https://doi.org/10.1002/pc.26504

[10] F. Mirhoseini, Alireza Salabat, Removal of methyl tert -butyl ether as a water pollutant by photodegradation over a new type of poly(methyl methacrylate)/$TiO_2$ nanocomposite. Polymer Composites, 39(4) (2018) 1248–1254. https://doi.org/10.1002/pc.24059

[11] A. Salabat, F. Mirhoseini, Applications of a new type of poly(methyl methacrylate)/$TiO_2$ nanocomposite as an antibacterial agent and a reducing photocatalyst. Photochem. Photobiol. Sci., 14(9) (2015) 1637–1643. https://doi.org/10.1039/c5pp00065c

[12] F. Mirhoseini, Alireza Salabat, Investigation of operational parameters on the photocatalytic activity of a new type of poly(methyl methacrylate)/ionic liquid-$TiO_2$ nanocomposite, Iranian J. Chem. Chem. Eng., 38 (2019) 101-114. https://doi.org/10.30492/IJCCE.2019.37613

[13] A. Salabat, F. Mirhoseini, F.H. Nouri, Microemulsion strategy for preparation of $TiO_2$–Ag/poly(methyl methacrylate) nanocomposite and its photodegradation application. J. Iranian Chem. Soc. 20 (2022) 599–608. https://doi.org/10.1007/s13738-022-02693-7.

[14] F. Mirhoseini, A. Salabat, Polymer nanocomposite based composition and method for controlling water hardness, United States patent 11136247

[15] A. Salabat, F. Mirhoseini, M. Mahdieh, H. Saydi, A novel nanotube-shaped polypyrrole-Pd composite prepared using reverse microemulsion polymerization and its evaluation as an antibacterial agent, New J. Chem. 39 (5) (2015) 4109–4114. https://doi.org/10.1039/c5nj00175g

[16] A. Salabat, F. Mirhoseini, M. Arjomandzadegan, E. Jiryaei, A novel methodology for fabrication of Ag-polypyrrole core-shell nanosphere using microemulsion system and evaluation of its antibacterial application, New J. Chem. 41 (21) (2017) 12892–12900. https://doi.org/10.1039/c7nj00678k

[17] F. Mirhoseini, A. Salabat, Antibactrial activity based poly(methyl methacrylate) supported $TiO_2$ photocatalyst film nanocomposite, Tech. J. Eng. Appl. Sci. 5 (2015)115-118.

[18] P. Assefi, M. Ghaedi, A. Ansari, M.H. Habibi, M.S. Momeni, Artificial neural network optimization for removal of hazardous dye Eosin Y from aqueous solution using $Co_2O_3$-NP-AC: Isotherm and kinetics study. J Ind Eng Chem. 2014; 20: 2905–2913. https://doi.org/10.1016/j.jiec.2013.11.027

[19] R. Hosseini Nia, M. Ghaedi, A.M. Ghaedi, Modeling of reactive orange 12 (RO 12) adsorption onto gold nanoparticle-activated carbon using artificial neural network optimization based on an imperialist competitive algorithm. J Mol Liq. 2014; 195: 219–229. https://doi.org/10.1016/j.molliq.2014.02.026

[20] H. Karimi, M. Ghaedi. Application of artificial neural network and genetic algorithm to modeling and optimization of removal of methylene blue using activated carbon. J Ind Eng Chem. 2014; 20: 2471–2476. https://doi.org/10.1016/j.jiec.2013.10.028

[21] A. M. Ghaedi, A. Vafaei, Applications of artificial neural networks for adsorption removal of dyes from aqueous solution: A review, Adv. Colloid Interface Sci, 2017. https://doi.org/10.1016/j.cis.2017.04.015

[22] F. Mirhoseini, A. Salabat, Ionic liquid based microemulsion method for fabrication of poly(methyl methacrylate)–$TiO_2$ nanocomposite as highly efficient visible light photocatalyst, RSC Adv. 5 (2015) 12536–12545. https://doi.org/10.1039/c4ra14612c

[23] F. Mirhoseini, Alireza Salabat, Photocatalytic filter, United States patent 10828629.

[24] A. Zolanvari, H. Sadeghi, J. Nezamdost, K. Suratgar, High Temperature X-Ray Diffraction and Fuzzy Modeling of Ni/Cu Multilayers, J Mater Sci Eng. 5(4) (2011) 386.

[25] A.A. Suratgar, S.K. Nikravesh, Potential energy based stability analysis of fuzzy linguistic systems, Iranian J. Fuzzy Systems, 2(1) (2005) 65-74.

[26] N.K. Kasabov, Foundation of neural networks, fuzzy systems and knowledge engineering, The MIT press, London, England, 1998.

[27] K. Samarjit, S. Das, P. Kanti Ghosh. Applications of neuro fuzzy systems: A brief review and future outline. Appl Soft Comput. 2014; 15: 243–259. https://doi.org/10.1016/j.asoc.2013.10.014

[28] S.I. Park, J.H. Lim, C.O. Kim. Surface-modified magnetic nanoparticles with lecithin for applications in biomedicine. Curr Appl Phys. 2008; 8: 706–709. https://doi.org/10.1016/j.cap.2007.05.009
[29] F. Kamali, K. Faghihi, F. Mirhoseini, High antibacterial activity of new eco-friendly and biocompatible polyurethane nanocomposites based on $Fe_3O_4$/Ag and starch moieties. Polym. Eng. Sci., 62(5) (2022) 1444-1462.https://doi.org/10.1002/pen.25934
[30] A. Salabat, F. Mirhoseini, R. Valirasti, Engineering poly(methyl methacrylate)/$Fe_2O_3$ hollow nanospheres composite prepared in microemulsion system as a recyclable adsorbent for removal of benzothiophene, Ind. Eng. Chem. Research 58 (2019) 17850-1785. https://doi.org/10.1021/acs.iecr.9b04322
[31] J. Zolgharnein, M. Bagtash, N. Asanjarani, Chemometrics approach for optimization of simultaneous adsorption of Alizarin red S and Congo red by cobalt hydroxide nanoparticles. J Chemometr. 2017. https://doi.org/10.1002/cem.2886
[32] M. Khajeh, A. Barkhordar, Modelling of solid-phase tea waste extraction for the removal of manganese from food samples by using artificial neural network approach, Food Chem. 141 (2013) 712–717. https://doi.org/10.1016/j.foodchem.2013.04.075
[33] J. Zolgharnein, N. Asanjrani, M. Bagtash, G. Azimi, Multi-response optimization using Taguchi design and principle component analysis for removing binary mixture of alizarin red and alizarin yellow from aqueous solution by nano γ-alumina, Spectrochim Acta A. 126 (2014) 291–300. https://doi.org/10.1016/j.saa.2014.01.100